NASA TECHNICAL REPORT

NASA TR R-239

MONTE CARLO INTERPRETATION OF SPHERE TRANSMISSION EXPERIMENTS FOR AVERAGE CAPTURE CROSS SECTIONS AT 24 KEV

by Donald Bogart and Thor T. Semler

Lewis Research Center
Cleveland, Ohio

NATIONAL AERONAUTICS AND SPACE ADMINISTRATION • WASHINGTON, D. C. • JUNE 1966

NASA TR R-239

MONTE CARLO INTERPRETATION OF SPHERE TRANSMISSION EXPERIMENTS FOR AVERAGE CAPTURE CROSS SECTIONS AT 24 KEV

By Donald Bogart and Thor T. Semler

Lewis Research Center
Cleveland, Ohio

NATIONAL AERONAUTICS AND SPACE ADMINISTRATION

For sale by the Clearinghouse for Federal Scientific and Technical Information
Springfield, Virginia 22151 – Price $1.00

MONTE CARLO INTERPRETATION OF SPHERE TRANSMISSION EXPERIMENTS FOR AVERAGE CAPTURE CROSS SECTIONS AT 24 KEV*

by Donald Bogart and Thor T. Semler

Lewis Research Center

SUMMARY

Monte Carlo analyses of sphere transmission experiments at 24 keV are made by using statistical results from slow neutron resonance spectroscopy as input data. An average capture cross section $\overline{\sigma}_C$ for gold of 700±50 millibarns is obtained compared with a reported value of 532±60 millibarns evaluated by a widely used multiple scattering analysis. A small p-wave contribution is required for gold. For iodine s-wave and p-wave contributions of 442±50 and 358±60 millibarns, respectively, provide a $\overline{\sigma}_C$ of 800±80 millibarns. This value is in substantial agreement with a reported value of 768±90 millibarns. For nuclei with large s-wave scattering, such as gold, the usual multiple scattering analysis is shown to encounter difficulties because of ambiguity as to the effective scattering cross section to be used.

INTRODUCTION

The spherical shell transmission method has been used with antimony-beryllium neutron sources by Schmitt and Cook (ref. 1) to measure the absolute value of average capture cross section for several elements. The capture cross sections for five of these elements (gold, iodine, indium, antimony, and silver) were used in a group normalization by Gibbons, Macklin, Miller, and Neiler (ref. 2) to place the large fund of keV capture data measured with the liquid scintillator tank on an absolute basis. Because of the longstanding discrepancies in the capture cross sections for gold in the keV region (ref. 3), this study was undertaken to investigate the validity of the method used to analyze sphere transmission data at 24 keV. A source of discrepancy for capture cross

*Presented at Conference on Neutron Cross Section Technology, Washington, D. C., March 22-24, 1966.

sections in the keV region due to probable errors in the cross sections of boron 10 has been discussed (ref. 4).

The capture cross section obtained from analysis of the sphere transmission experiment is an average over the statistical distributions of the unresolved resonances in the energy interval defined by neutrons emitted from the source. The energy of neutrons from the antimony-beryllium source was determined by Schmitt (ref. 5) to be 24.0±2.2 keV. For medium-weight and heavy nuclei, the average spacing of resonances is approximately 10 electron volts, so that several hundred levels are sampled by the source neutrons in traversing the sphere. An accurate interpretation of the multiple scattering processes is required to relate the observed transmission to the average capture cross section. The effects of resonance scattering must be taken into consideration.

The general problem of determining slowly varying inelastic cross sections in the MeV region from sphere transmission measurements has been analyzed by Bethe, Beyster, and Carter (ref. 6). This method of analysis, which was used by Schmitt, assumes that capture and scattering cross sections are energy independent in the keV region, but it does include the multiple scattering processes explicitly. The effects of the statistically spaced levels with varying capture and resonance scattering cross sections superimposed on a potential scattering base are not considered explicitly by Schmitt. The resonance structure of the cross sections was considered only in relatively large resonance self-protection corrections that are applied to average capture cross sections obtained by the Bethe method of analysis.

In order to illustrate some limitations of these sphere analyses, several idealized sphere transmission problems have been computed by a Monte Carlo method. These illustrative calculations employ several arbitrary step scattering and capture cross sections. The spacings and magnitudes of the steps are such as to provide the same average value of capture cross section as for a nucleus possessing constant scattering and capture cross sections.

A direct Monte Carlo analysis of the sphere transmission experiments has been performed for iodine and for gold. In the Monte Carlo analysis, the average s-wave contribution is calculated by using as input data both the Doppler-broadened Breit-Wigner resonance cross sections computed from published statistical results on reduced neutron width distributions and the level spacing distributions obtained from slow neutron resonance spectroscopy.

SYMBOLS

D level spacing

E neutron energy

E_0	resonance energy
g	spin weight factor, $(2J + 1)/[2(2I + 1)]$
I	target nucleus spin
J	compound nucleus spin
ℓ	orbital angular momentum parameter
N	atom density
R'	effective nuclear radii
r_1	inner sphere radius
r_2	outer sphere radius
T	transmission
(1-T)	capture fraction
σ_C	capture cross section
σ_{C_p}	p-wave capture cross section
σ_{C_s}	s-wave capture cross section
σ_{pot}	potential scattering cross section
σ_{S_s}	s-wave resonance scattering cross section
σ_T	total cross section
Γ	total width
Γ_n	neutron width
Γ_γ	radiation width

LIMITATIONS OF SPHERE TRANSMISSION ANALYSIS

The measurements of average capture cross sections by the shell transmission method employ thick spherical shells of the materials studied. These shells contain a centrally located compact source of 24-keV neutrons that make multiple collisions with the shell material and are either captured or transmitted. A measurement of the count-rate ratio using an external flat response neutron detector with the shell in place and with the shell removed determines the shell transmission. For neutrons in the kilovolt re-

gion, only elastic scattering and capture processes occur. If cross sections are constant, and the average scattering cross section is known, the average capture cross section may be calculated by the multiple scattering model. It is shown that for cross sections that vary with energy, the analytical model can be in error.

Sphere Analysis With Energy-Independent Cross Sections

The analytical model that has been used is equivalent to the thick shell theory of Bethe, et al. (ref. 6). This theory was developed to interpret sphere transmission experiments for measuring average inelastic scattering cross sections.

This method of sphere transmission analysis, which Bethe tested for many cases by a Monte Carlo analysis, employs separate escape probabilities from a spherical shell after isotropic elastic scattering on the first and second collisions. After the second collision, the neutrons are taken to be distributed in random directions, according to a spatial normal mode, so that the effects on transmission of the third and all subsequent collisions are combined into a single escape probability. The shell thickness is assumed to be of the order of one total mean free path so as to satisfy the requirement that the density of neutrons from the source shall not fall off too much from the inside of the shell to the outside. The shells used in the sphere transmission measurements (ref. 1) varied from one-half to two average total mean free paths in thickness. For iodine and gold, shell thicknesses in mean free paths can be twice these values and more for Doppler-broadened cross sections because of resonance scattering contributions. Resonance fluxes for first-collided and multiply-collided neutrons attenuate by local values of scattering cross section that are larger than the average value of scattering cross section.

The resonance shapes of scattering and capture cross sections at 24 keV have been considered only in relatively large self-protection corrections that are applied to the results obtained from the Bethe analysis. As discussed by Schmitt (ref. 7), the problem of calculating resonance self-protection corrections for spherical shells is a formidable one, and the limited progress made in this direction for thin disk samples is cited. The evaluation of resonance self-protection corrections in the kilovolt region requires independent data on average s- and p-wave resonance parameters and level spacings, whereas one of the ostensible reasons for measuring average capture cross sections in the keV region has been the determination of s- and p-wave strength functions in the unresolved energy region.

Several idealized problems have been computed for typical spheres by using a Monte Carlo method in order to explore some limitations of the Bethe formulation. The Monte Carlo code assumes a monoenergetic and isotropic point source of neutrons centrally located in a spherical shell. The multiple collision paths of these neutrons are followed

through the shell until the neutron is either absorbed or transmitted. On elastic collision, the neutron is scattered isotropically in the center-of-mass system. For medium-weight and heavy nuclei, it is a reasonable and a convenient simplification if elastic scattering is taken to be isotropic in the laboratory system as well. The average energy a neutron may lose in an elastic collision is from 1 to 2 percent of its energy; at 24 keV, this energy loss is very much greater than the average level spacing.

The spatial aspects of the Monte Carlo method used are similar to those described by Everett, Cashwell, and Rechard (ref. 8), and they take into account the exact geometric and angular coordinates in all collisions. As a check on the present Monte Carlo code, a particular sphere transmission problem has been solved that is very similar to a Monte Carlo calculation cited by Bethe, who also used the method of Everett. (This problem is case 9 of table 4.1 on p. 275 of ref. 6.) The conditions of the problem are as follows:

Total cross section, σ_T, b	3.17
Capture cross section, σ_C, b	0.72
Sphere thickness in total mean free paths, $N\sigma_T(r_2 - r_1)$	2.465
Ratio of inner to outer sphere radius, r_1/r_2	0.094
Bethe Monte Carlo transmission, T	0.405
Present Monte Carlo transmission, T	0.4061

The present Monte Carlo calculation followed 25 000 neutron histories, and the two transmission values are in excellent agreement.

Sphere Analysis With Step Cross Sections

The present Monte Carlo analysis is readily adaptable to the study of the effects of variable cross sections on transmission through specific spheres. Illustrative calculations are made that employ several arbitrary step scattering and capture cross sections adjusted to provide the same average values of capture cross section.

The cross section shapes used are shown in figure 1. The constant capture cross section σ_C and the potential scattering cross section σ_{pot} are shown in figure 1(a). The repetitive step capture cross section over a level spacing D is shown in figure 1(b) with a window fraction f defined as that fraction of D that is devoid of capture. Finally, the repetitive step in both capture cross section and scattering cross section σ_S is shown in figure 1(c).

The dimensions and density of the thick gold sphere and the iodine sphere employed by Schmitt and Cook (ref. 1) were used in these Monte Carlo calculations. The results

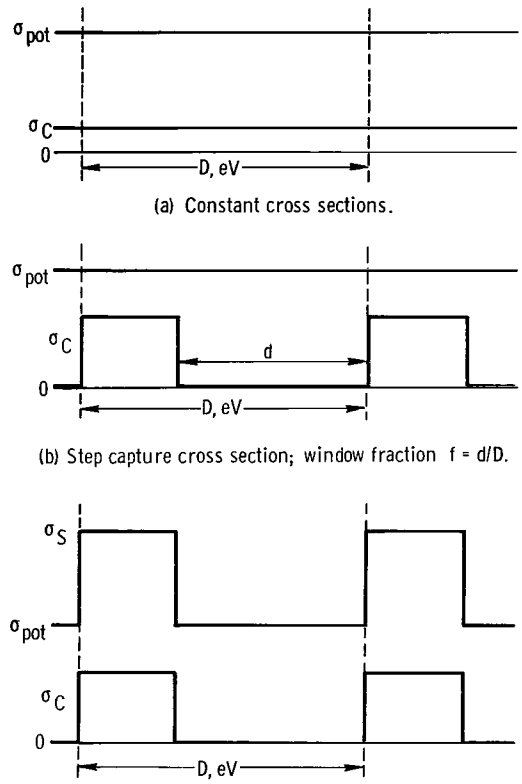

Figure 1. - Cross sections used for illustrative Monte Carlo sphere transmission calculations.

for gold are shown in figure 2(a) and are plotted as the nontransmission or capture fraction (1 - T) as a function of the average capture cross section $\overline{\sigma}_C$. The uppermost curve corresponds to the Bethe calculation, that is, a window fraction f of zero. The present Monte Carlo values for f of zero are in excellent agreement with this curve. The other three solid lines are for the same constant scattering cross section and values of $\overline{\sigma}_C$ but for different values of f. As f increases, the capture fraction (1 - T) decreases. Finally, the two dashed lines are for the cases illustrated by figure 1(c). As additional step scattering is added, the capture fraction decreases further.

The value of (1 - T) for this gold sphere was measured in reference 1 as 0.200 and is shown in figure 2(a) to have a $\overline{\sigma}_C$ of 0.500 barn for the assumed constant potential scattering cross section of 12 barns. However, all values of $\overline{\sigma}_C$ that consider the resonance nature of the cross sections as represented by the stepped values are larger than the values for f of zero.

The comparable Monte Carlo results for the iodine sphere are shown in figure 2(b). The uppermost curve corresponds to the Bethe formulation. The other two solid lines are for the same constant scattering cross sections but for different values of f. The dashed line shows the results for the cases illustrated by figure 1(c). As noted before, the capture fraction decreases as f is increased or as resonance scattering is added.

The value of (1 - T) for this iodine sphere was measured in reference 1 as 0.077 and is shown in figure 2(b) to have a $\overline{\sigma}_C$ of 0.800 barn for the assumed constant potential scattering cross section of 5 barns. Once again, all values of $\overline{\sigma}_C$ that consider the resonance character of the cross sections as represented by the steps are larger than the values for f of zero.

The effects shown in figure 2 are more easily visualized for two extreme cases, that of a window fraction f of zero and that of a value of f near one. For an f of zero, the capture fraction may be calculated directly by the Bethe formulation, and a consistent value of $\overline{\sigma}_C$ is obtained. However, as a window fraction of unity is approached, the step value of σ_C corresponds to a local capture cross section that is becoming infinite. Inasmuch as the neutrons that interact with this capture cross section are attenuated exponen-

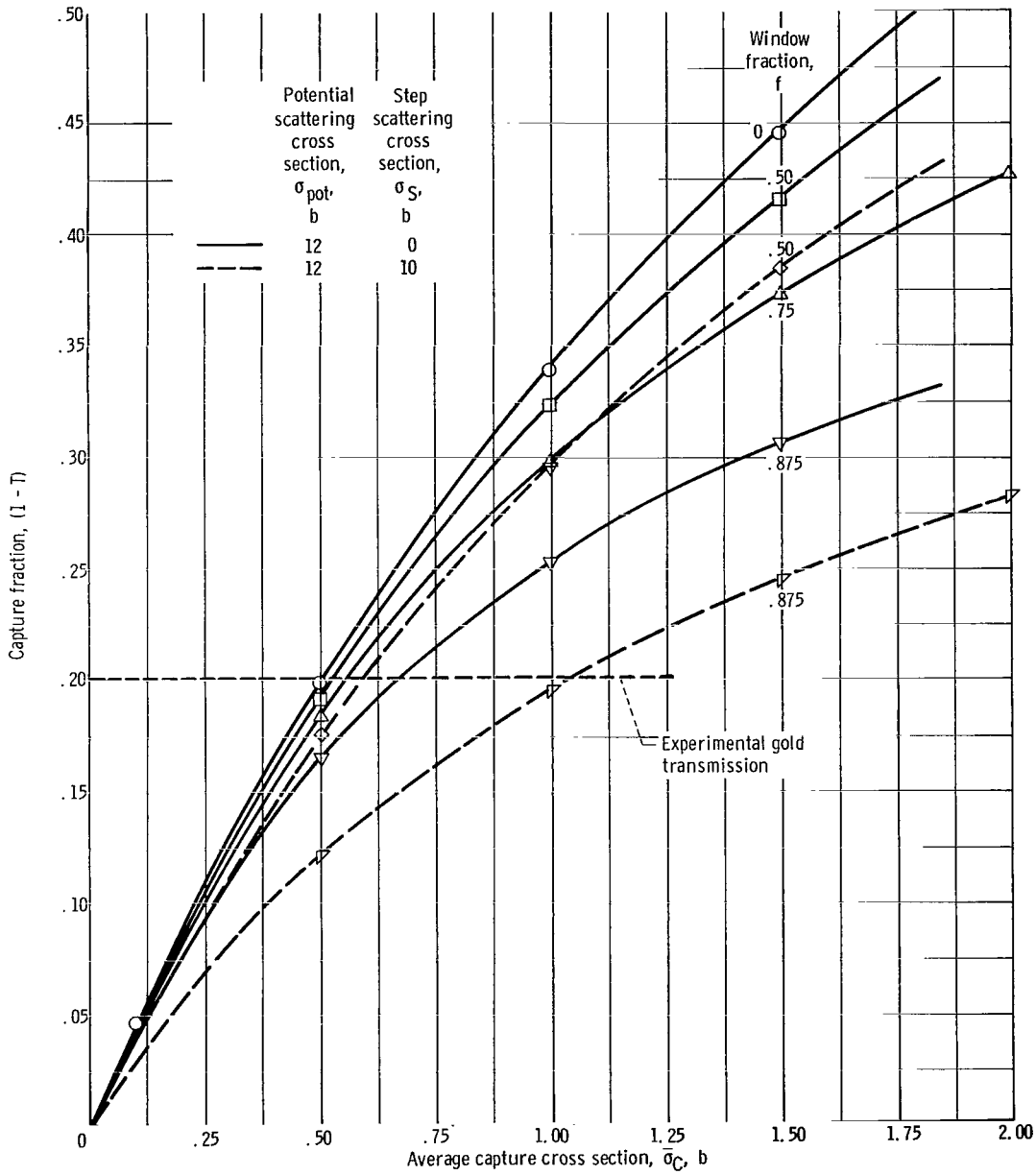

(a) Gold sphere 2.

Figure 2. - Monte Carlo calculations for gold and iodine spheres using step changes in cross sections.

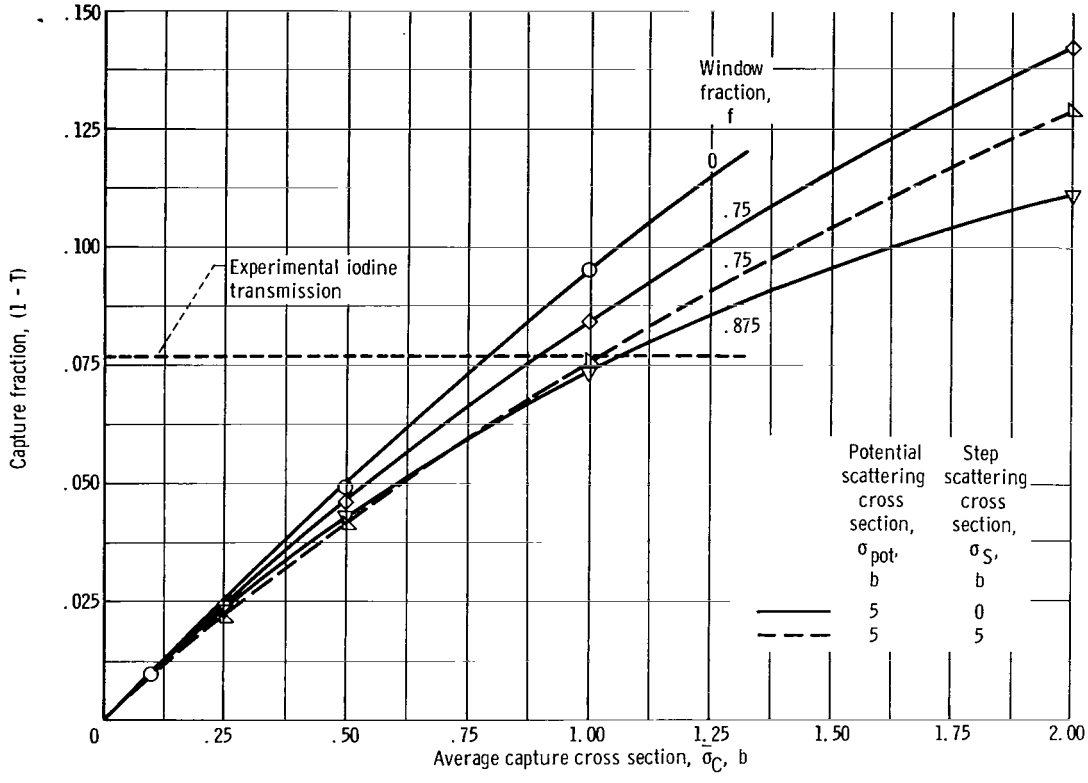

(b) Iodine sphere.

Figure 2. - Concluded.

tially, the value of the capture fraction approaches zero.

The results shown in figure 2 beg the question as to how the reported results of references 1 and 7, which use resonance self-protection corrections that are applied to the Bethe analysis, compare with a quantitative interpretation of the sphere transmission experiments. In order to execute a direct Monte Carlo interpretation of the sphere transmission experiments, the pertinent statistical data on level widths and level spacings at 24 keV must be known. Available input data for iodine and for gold are discussed in the following section.

CROSS SECTIONS AND CAPTURE INTEGRALS AT 24 KEV

The discussion and analysis that follow are restricted to the isotopes iodine 127 and gold 197 because they were measured by Schmitt and Cook (ref. 1) and because good statistical data on their reduced neutron widths and level spacings are available. Furthermore, these isotopes are 100-percent abundant in their natural state and are representative of the medium-weight and heavy nuclei.

Iodine

Total neutron cross section measurements have been made recently for iodine and other elements by Garg, et al. (ref. 9) with an energy resolution higher than previously possible. Up to 4 keV, 290 levels were observed in transmission measurements.

After excluding apparent p-wave levels, the distribution of adjacent s-wave level spacings D was found to follow a single-population Wigner distribution given by

$$P\left(\frac{D}{\overline{D}}\right) = \frac{\pi}{2}\frac{D}{\overline{D}}e^{-\pi D^2/4\overline{D}^2}$$

The average s-wave level spacing $\overline{D}$ was found to be 13.5±0.5 electron volt. Analysis of the resolved s-wave levels provides a weighted average radiation width $\overline{\Gamma}_\gamma$ of 0.107 electron volt. The observed distribution of neutron widths Γ_n for s-wave resonances was analyzed and the reduced widths $\Gamma_n^o = \Gamma_n/E_0^{1/2}$, where E_0 is the resonance energy, were found to follow a chi-squared distribution with 1 degree of freedom. This distribution, known as the Porter-Thomas distribution, is given by a frequency function of the form

$$P(x) = \frac{1}{\sqrt{2\pi}}x^{-1/2}e^{-x/2}$$

where x is equal to $\Gamma_n^o/\overline{\Gamma}_n^o$, and $\overline{\Gamma}_n^o$ is the average reduced width in the population sample. The value of $\overline{\Gamma}_n^o$ selected by Garg for s-wave iodine levels is 0.84±0.15 millivolt. The s-wave strength function S_0 was reported as

$$S_0 = \frac{\overline{\Gamma}_n^o}{\overline{D}} = 0.62\pm0.09\times10^{-4}$$

Gold

For gold, total cross section measurements have been made by Desjardins, Rosen, Havens, and Rainwater (ref. 10), who analyzed data for 88 observed spacings to 1566 electron volts and reported resonance parameters for 55 levels to 940 electron volts. The level spacing distribution was found to agree somewhat better with a two-population rather than with a single-population Wigner distribution. An average level spacing $\overline{D}$

of 16.8 electron volts was obtained. Analysis of the resolved s-wave resonances provided a weighted average radiation width $\overline{\Gamma}_\gamma$ of 0.170 electron volt for gold.

The distribution of reduced neutron widths was found to follow the Porter-Thomas single-population function. The value for the s-wave strength function was reported as

$$S_0 = \frac{\overline{\Gamma}_n^0}{\overline{D}} = 1.5 \pm 0.3 \times 10^{-4}$$

Representative Cross Sections at 24 keV

The number of p-wave resonances detected in these total cross section measurements for iodine and gold was insufficient to deduce average p-wave resonance parameters. However, an estimate of these may be made so as to illustrate the shape and magnitude of representative p-wave resonances relative to average s-wave resonances. A comparison of Doppler-broadened resonances at 24 keV is helpful as an indication of the much larger scattering cross section variation of s-wave relative to p-wave resonances.

The reduced neutron width for neutrons of orbital angular momentum ℓ is given by

$$\Gamma_n^\ell = \frac{\Gamma_n}{\nu_\ell E_0^{1/2}}$$

where ν_ℓ is the neutron penetrability factor arising from the centrifugal potential barrier. For $\ell = 0$, $\nu_0 = 1$; for $\ell = 1$,

$$\nu_1 = \frac{y^2}{1 + y^2}$$

where y is equal to $A^{1/3}E^{1/2}/3250$, and A is the atomic mass number.

Values of p-wave strength function S_1 for iodine and gold that were inferred from capture data by Gibbons (ref. 2) are used. Values of S_1 of $3.0 \pm 1.5 \times 10^{-4}$ for iodine and $0.3 \pm 0.3 \times 10^{-4}$ for gold are used.

Doppler-broadened cross sections at 24 keV for average resonances of iodine and gold at 293° K have been computed. These cross sections were computed with a FORTRAN IV code that was based on equations given in reference 11. The parameters used are listed in table I; the same value of $\overline{\Gamma}_\gamma$ has been used for both s- and p-wave levels. The values of potential scattering cross section σ_{pot} used are also listed.

TABLE I. - AVERAGE RESONANCE PARAMETERS AT 24 KEV

Isotope	Average radiation width, $\overline{\Gamma}_\gamma$, mV	Average s-wave level spacing, $\overline{D}$, eV	Average s-wave neutron width, $\overline{\Gamma}_{n_0}$, mV	Average p-wave neutron width, $\overline{\Gamma}_{n_1}$, mV	Potential scattering cross section, σ_{pot}, b
Iodine 127	107	13	280	60	4
Gold 197	170	17	760	15	12

The Doppler-broadened cross sections for average isolated levels at 24 keV and 293° K are shown in figure 3 for iodine and gold. For s-wave levels, large resonance scattering contributions are present, whereas for p-wave levels resonance scattering is small.

The peak s-wave cross sections of average Doppler-broadened resonances are indicated to be some 50 percent larger than σ_{pot} for iodine and to be about double that of σ_{pot} for gold. Significant interference between potential and resonance scattering is noted. For resonances with the larger neutron widths in the statistical distributions, these s-wave peaks and interference effects are even larger.

Resonance Capture Integral

The importance of levels with large neutron widths in the keV region may be illustrated by a calculation of the resonance capture integral. In this case, the resonance capture integral is the capture area under each resonance summed cumulatively over the resonances that comprise a normalized Porter-Thomas distribution.

The resonance capture integral I_0 for an isolated level in barns is given by

$$I_0 = 4090\ g \frac{\Gamma_n \Gamma_\gamma}{\Gamma E_0^2}$$

The s-wave resonance capture integral for a normalized Porter-Thomas distribution is then

$$\int_{x=0}^{\infty} P(x) I_0(x) dx \approx \sum_{i=1}^{n} P(x_i) I_0(x_i) \Delta x_i$$

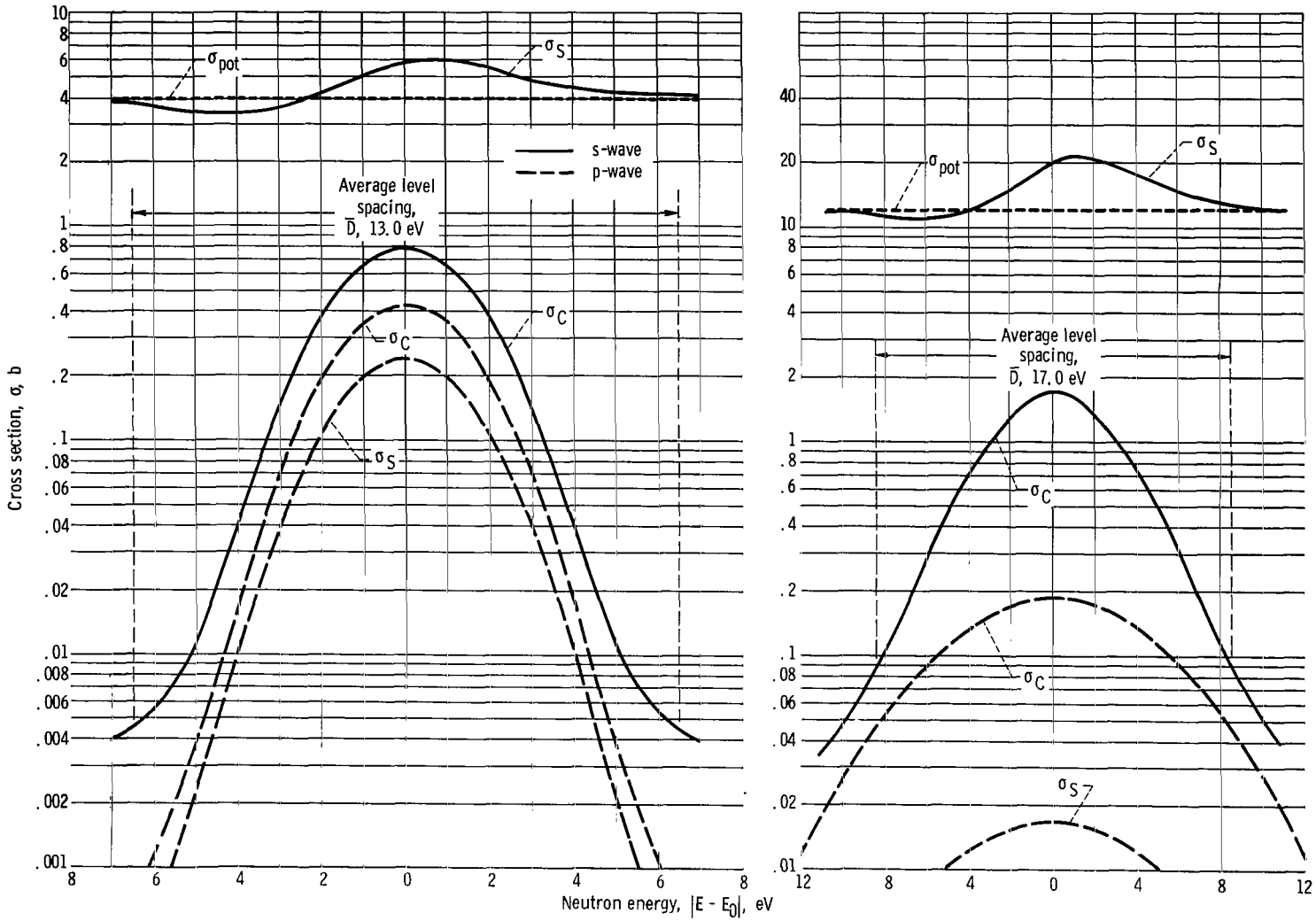

(a) Iodine resonance. Average radiation width, 107 millivolts; average s-wave neutron width, 280 millivolts; average p-wave neutron width, 60 millivolts; potential scattering cross section, 4 barns.

(b) Gold resonance. Average radiation width, 170 millivolts; average s-wave neutron width, 760 millivolts; average p-wave neutron width, 15 millivolts; potential scattering cross section, 12 barns.

Figure 3. - Doppler-broadened cross sections for average iodine and gold resonances at 24 keV and 293° K.

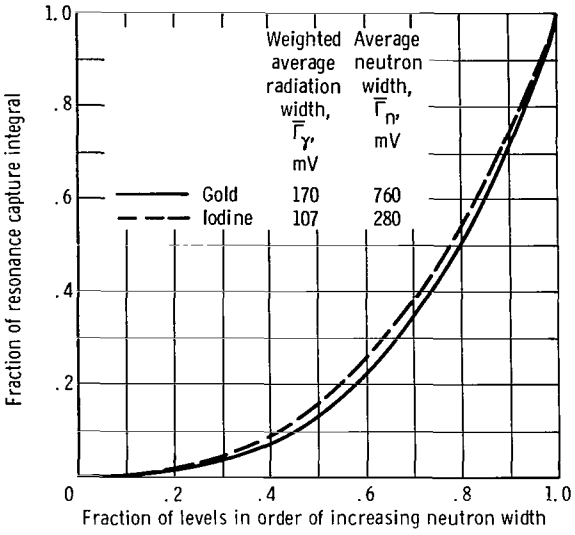

Figure 4. - Cumulative s-wave resonance capture integrals for normalized Porter-Thomas distribution of neutron widths for gold and iodine.

where

$$\sum_{i=1}^{n} \Delta x_i = 10$$

and

$$\int_{x=10}^{\infty} P(x)dx = 0.0008$$

The fraction of the s-wave resonance capture integral as a fraction of the levels in the order of increasing neutron width is shown in figure 4 for gold and iodine. The slow rise of the curves indicates that the levels with the smaller neutron widths make negligible contributions to resonance capture. The shapes of the curves indicate that the relatively fewer levels possessing the larger neutron widths make the largest contribution to resonance capture. Fifty percent of the resonance capture integral is contributed by about 20 percent of the levels with the larger neutron widths, and 85 percent of the resonance capture integral is contributed by about 50 percent of the levels with the larger neutron widths.

Statistical Distributions Used in Monte Carlo Calculations

For purposes of machine calculation, the Porter-Thomas distribution of reduced neutron widths is represented by 10 groups; each group width is the average of a decile of the normalized population. Each of these 10 values is then equally probable and serves to represent the distribution of neutron widths for the resonances in the energy region about 24 keV. The average neutron widths and the 10 values used for iodine and gold are listed in table II. With these values and in conjunction with the average values of $\bar{\Gamma}_\gamma$ cited in table I, tables of Doppler-broadened single-level Breit-Wigner resonances at 293° K are generated in the range from $E_0 = -50$ to $E_0 = +50$ electron volts in increments of 0.50 electron volt about a value of E_0 of 24 keV. The 2010 values of resonance scattering and resonance absorption cross sections are stored and are accessible to the Monte Carlo program. Completely new sets of values are computed if the value of the potential cross section is changed to include consistent interference effects between resonance and potential scattering for s-wave neutrons.

TABLE II. - GROUP REPRESENTATION OF PORTER-THOMAS DISTRIBUTION AT 24 KEV FOR IODINE AND GOLD

Population range	Group-to-average neutron width ratio, $\Gamma_n/\overline{\Gamma}_n$	Iodine neutron width, Γ_n, mV	Gold neutron width, Γ_n, mV
0.00 to 1.00	1.0000	280.0	760.0
0.00 to 0.10	0.0100	2.8	7.6
.10 to .20	.0435	12.2	33.0
.20 to .30	.1100	30.8	83.6
.30 to .40	.2435	68.2	185.0
.40 to .50	.3645	102.0	277.0
.50 to .60	.5805	162.5	441.2
.60 to .70	.8900	249.2	676.4
.70 to .80	1.3400	375.2	1018.4
.80 to .90	2.0700	579.6	1573.2
.90 to 1.00	4.3000	1204.0	3268.0

TABLE III. - GROUP REPRESENTATION OF WIGNER DISTRIBUTION AT 24 KEV FOR IODINE AND GOLD

Population range	Group-to-average level spacing ratio, $D/\overline{D}$	Iodine level spacing, D, eV	Gold level spacing, D, eV
0.00 to 1.00	1.000	13.0	17.0
0.00 to 0.10	0.267	3.5	4.5
.10 to .20	.450	5.5	8.0
.20 to .30	.590	7.5	10.5
.30 to .40	.710	9.0	12.5
.40 to .50	.860	11.0	15.0
.50 to .60	.980	12.5	17.0
.60 to .70	1.115	14.5	19.5
.70 to .80	1.313	17.0	22.5
.80 to .90	1.546	20.0	26.5
.90 to 1.00	2.137	28.0	36.5

The Wigner distribution of resonance level spacings is represented by 10 groups; each group level is the average of a decile of the population. Each of these 10 values is then equally probable and serves to define the level spacings for the resonances in the energy region about 24 keV. The average level spacings and the 10 values used for iodine and gold are listed in table III. The energy region is divided into intervals of 0.50 electron volt.

The Monte Carlo program operates in the following manner:

(1) A level spacing D is chosen at random from the 10 equally probable values.

(2) A resonance neutron width Γ_n is chosen at random from the 10 equally probable values.

(3) A second resonance neutron width is chosen at random from the 10 equally probable values.

(4) An energy interval in the spacing between the two selected resonances is chosen at random.

(5) The total cross section at this energy is evaluated as the sum of the contributions of the scattering and capture cross sections of the two nearest resonances less the value of the potential cross section σ_{pot}.

(6) If p-wave resonances are to be considered, the p-wave contribution σ_{C_p} is approximated as an additive constant.

TABLE IV. - AVERAGE s-WAVE CONTRIBUTION TO CAPTURE CROSS SECTION AS FUNCTION OF NEUTRON ENERGY

Energy, E, keV	Average s-wave capture cross section, σ_{C_s}, b	
	Iodine	Gold
2	3.800	5.457
24	.442	.665
200	.075	.073

TABLE V. - EFFECT OF GROUP REPRESENTATION OF NEUTRON WIDTHS AND LEVEL SPACINGS IN GOLD

Number of groups for neutron widths, Γ_n	Number of groups for s-wave level spacing, D	Average s-wave capture cross section, $\overline{\sigma}_{C_s}$, b
1	1	0.7216
5	1	.5560
10	1	.5206
1	1	.7216
1	5	.7184
1	10	.7202
1	1	.7216
5	5	.6734
10	10	.6640

It may be seen that, if the average s-wave capture and scattering cross sections for the selected statistical distributions and resonance parameters are desired, the Monte Carlo repeated samplings n readily provide these averages as

$$\overline{\sigma}_{C_s} = \frac{\sum_{i=1}^{n} \sigma_{C_{s_i}}}{n} \quad \text{and} \quad \overline{\sigma}_{S_s} = \frac{\sum_{i=1}^{n} \sigma_{S_{s_i}}}{n}$$

where n is of the order of 10^5.

The Monte Carlo method has been used in this way to calculate the average s-wave contribution to capture $\overline{\sigma}_{C_s}$ as a function of neutron energy for iodine and gold by using σ_{pot} values of 4.0 barns for iodine and 9.0 barns for gold (see table IV).

The adequacy of representing the observed distributions of reduced neutron widths and level spacings by 10 groups has been tested numerically. The value of $\overline{\sigma}_{C_s}$ for gold was calculated by representing the observed distributions by a single average value, 5 groups, and 10 groups, in respective combinations. The results for gold are shown in table V.

The calculations show that 10 groups for both Γ_n and D adequately represent the statistical distributions. An interesting result is that it appears to be essential to consider simultaneously the distributions in Γ_n and D because their interaction affects the average s-wave capture cross section $\overline{\sigma}_{C_s}$.

In general, each Monte Carlo interpretation of a sphere transmission experiment follows 100 000 source neutrons. Depending on the thickness of the spherical shell, the

TABLE VI. - SPHERICAL SHELL TRANSMISSION DATA AT 24 KEV AND RESULTS OF SCHMITT AND COOK (REF. 1) AND SCHMITT (REF. 7)

Shell	Total cross section, $\bar{\sigma}_T$, b	Shell dimensions			Transmission, T	Average capture cross section, $\bar{\sigma}_C$, mb	
		Atom density, N, atom/cc	Inner sphere radius, r_1, cm	Outer sphere radius, r_2, cm		Uncorrected for resonance self-protection	Corrected for resonance self-protection
Iodine	6.69±0.36	0.01227×10^{24}	4.96	11.21	0.923±0.006	653±70	768±90
Gold 1	13.67±0.28	.0587	5.93	7.62	.876±0.005	495±52	532±60
Gold 2	13.67±0.28	.0587	5.08	7.62	.800±0.004	480±83	518±90
Indium	6.11±0.18	.0381	3.80	7.10	.853±0.005	794±36	854±60
Antimony	5.99±0.14	.0328	2.54	7.62	.873±0.005	509±27	578±45
Silver	7.85±0.23	.0581	4.30	7.46	.694±0.004	958±45	1127±80

TABLE VII. - MONTE CARLO RESULTS FOR IODINE AND GOLD

Sphere	Potential scattering cross section, σ_{pot}, b	Average s-wave capture cross section, $\bar{\sigma}_{C_s}$, b	Average p-wave capture cross section, $\bar{\sigma}_{C_p}$, b	Average s-wave resonance scattering component, $\bar{\sigma}_{S_s}$, b	Average total cross section, $\bar{\sigma}_T$, b	Transmission, T	Collisions per source neutron
Iodine	3.0	0.4426	0	1.831	5.274	0.9596	0.4330
	4.0	.4415	0	1.835	6.277	.9575	.5486
	5.0	.4427	0	1.847	7.290	.9555	.6830
	6.0	.4429	0	1.856	8.299	.9535	.8215
	4.0	.4415	.200	1.835	6.477	.9382	.5478
	4.0	.4415	.400	1.835	6.677	.9186	.5398
Gold 1	12.0	0.6641	0	4.265	16.929	0.8577	3.6625
	11.0	.6641	0	4.267	15.931	.8640	3.2770
	9.0	.6644	0	4.273	13.937	.8766	2.5508
	7.2	.6638	0	4.233	12.097	.8886	1.9580
	9.0	.6642	.100	4.278	14.042	.8561	2.4974
	9.0	.6648	.200	4.279	14.144	.8367	2.4455
Gold 2	12.0	0.6641	0	4.285	16.949	0.7733	5.9105
	11.0	.6645	0	4.273	15.938	.7844	5.2541
	9.0	.6638	0	4.227	13.891	.8075	4.0332
	7.2	.6640	0	4.261	12.125	.8263	2.9156
	9.0	.6647	.100	4.245	14.010	.7770	3.9101
	9.0	.6650	.200	4.259	14.124	.7489	3.8043

average number of collisions per source neutron varies from approximately 0.5 to approximately 6.0. While the program makes use of nonbiased sampling techniques, the convergence of results and the time of operation are quite rapid. The running time of the code for a moderately thick shell and 100 000 source neutrons is about 10 minutes on an IBM 7094 computer.

MONTE CARLO ANALYSIS OF SPHERE TRANSMISSION EXPERIMENTS

The pertinent shell transmission data that were measured and analyzed in reference 1 are given in table VI. Included in the table are the capture cross sections $\overline{\sigma}_C$ that were updated by Schmitt (ref. 7) for new experimental values of average total cross sections $\overline{\sigma}_T$ at 24.0 keV. Values of $\overline{\sigma}_C$ obtained were corrected for resonance self-protection (RSP) by factors that are as large as 15 percent.

The iodine and gold spheres listed in table VI have been analyzed by the present Monte Carlo method. The conditions to be satisfied simultaneously by the Monte Carlo calculations are the experimental values of $\overline{\sigma}_T$ and T. The constituent parts of $\overline{\sigma}_T$ are the s-wave and p-wave capture cross sections $\overline{\sigma}_{C_s}$ and $\overline{\sigma}_{C_p}$, the s-wave resonance scattering component $\overline{\sigma}_{S_s}$, and the potential scattering cross section σ_{pot}. In order to initiate the calculations, several values of σ_{pot} are selected.

Iodine

The Monte Carlo results for the iodine spherical shell are listed in table VII, which presents values of $\overline{\sigma}_{C_s}$, $\overline{\sigma}_{S_s}$, $\overline{\sigma}_T$, and T for several values of assigned σ_{pot} and $\overline{\sigma}_{C_p}$. The calculated s-wave component $\overline{\sigma}_{C_s}$ of 0.442 barn is inadequate to account for the observed value of T of 0.923 and indicates that a large p-wave component $\overline{\sigma}_{C_p}$ is required. This is shown in figure 5(a) in which T is plotted against $\overline{\sigma}_{C_p}$ for the four selected values of σ_{pot}. The essentially linear results for a σ_{pot} of 4.0 barns permit the dashed lines for the other values of σ_{pot} to be drawn.

The experimental value of transmission of 0.923±0.006 is indicated in figure 5(a). The calculated values of $\overline{\sigma}_T$ that satisfy the experimental value of T are found as $\overline{\sigma}_T = \overline{\sigma}_{C_s} + \overline{\sigma}_{C_p} + \overline{\sigma}_{S_s} + \sigma_{pot}$ for each value of σ_{pot}. These values of $\overline{\sigma}_T$ are plotted against σ_{pot} in figure 6(a), and the experimental value of $\overline{\sigma}_T$ of 6.69±0.36 barn is indicated. The value of σ_{pot} that satisfies both the measured values of $\overline{\sigma}_T$ and of T is

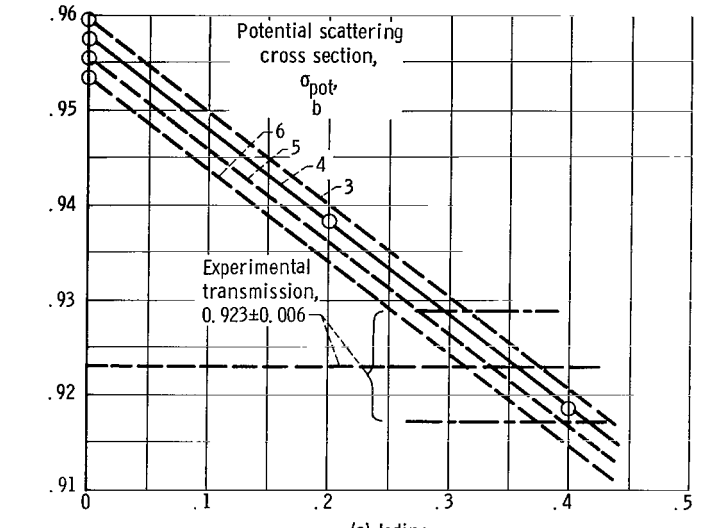

(a) Iodine.

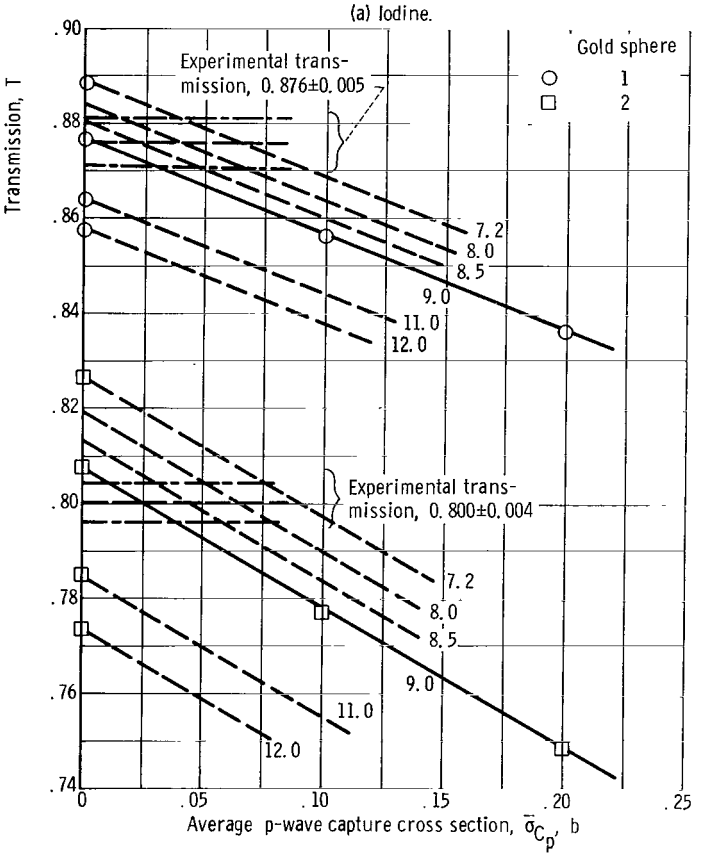

(b) Gold.

Figure 5. - Monte Carlo calculations for iodine and gold spherical shells.

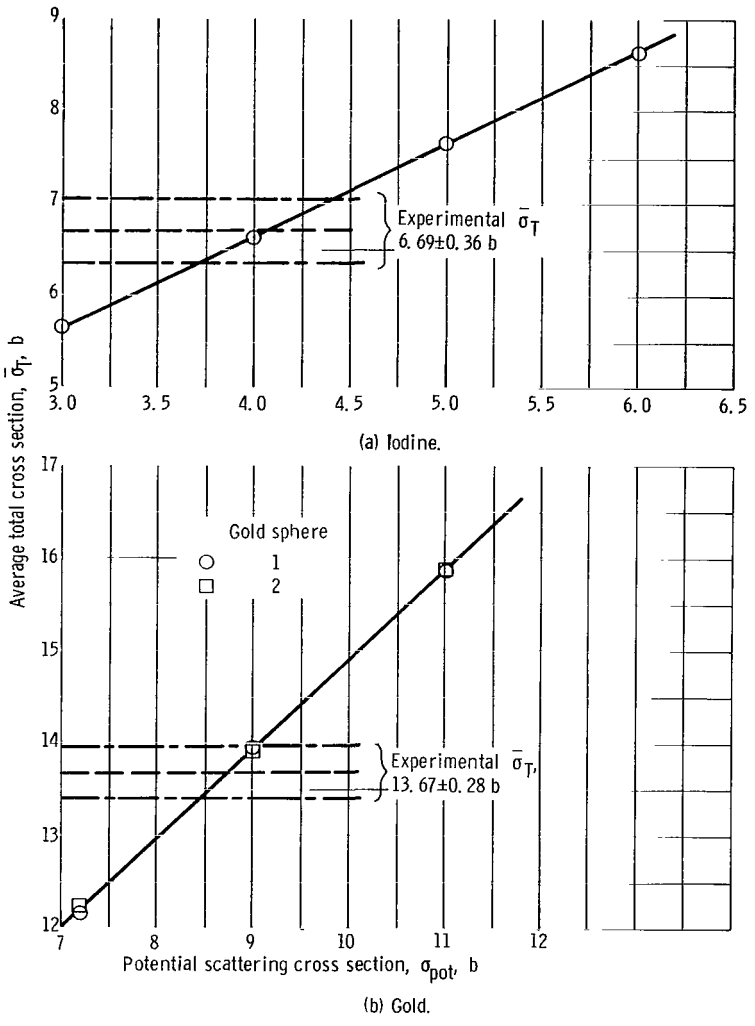

Figure 6. - Monte Carlo calculations for iodine and gold spherical shells that satisfy the most probable experimental transmissions.

4.0±0.3 barn. The consistent value of $\bar{\sigma}_{C_p}$ is obtained from figure 5(a) as 0.358±0.060 barn.

The average number of collisions per source neutron is also shown in table VII. For each case, 100 000 source neutrons were followed either to a transmission or to a capture. For the iodine sphere, about 82 000 collisions were tallied for a value of σ_{pot} of 6.0 barns.

The uncertainties in $\bar{\sigma}_{C_s}$, which result from uncertainties in the resonance parameters that are used as input data to the Monte Carlo analysis, are calculated separately. Both the effects on $\bar{\sigma}_{C_s}$ of an estimated 10-percent uncertainty in $\bar{\Gamma}_\gamma$ and the measured uncertainties in $\bar{\Gamma}_n$ and $\bar{D}$ that were cited earlier were evaluated by separate Monte Carlo calculations.

Interpretation of the sphere transmission experiment, which is consistent with the measured average total cross section and the known s-wave resonance parameters, provides the following cross sections for iodine: σ_{pot} = 4.0±0.3 barn; $\overline{\sigma}_{C_s}$ = 0.442±0.050 barn; $\overline{\sigma}_{C_p}$ = 0.358±0.060 barn; and $\overline{\sigma}_C$ = 0.800±0.080 barn.

Gold

The Monte Carlo results for the two gold spherical shells are listed in table VII, which presents values of $\overline{\sigma}_{C_s}$, $\overline{\sigma}_{S_s}$, $\overline{\sigma}_T$, and T for several assigned values of σ_{pot} and $\overline{\sigma}_{C_p}$. These results are shown in figure 5(b) in which T is plotted against $\overline{\sigma}_{C_p}$ for the various values of σ_{pot}.

The experimental values of transmission shown in figure 5(b) indicate that a small p-wave cross section is present. The calculated values of $\overline{\sigma}_T$ that satisfy these experimental values of T are plotted against σ_{pot} in figure 6(b), and the experimental value of $\overline{\sigma}_T$ of 13.67±0.28 barn is indicated. The value of σ_{pot} that satisfies the measured values of both $\overline{\sigma}_T$ and T is 8.7±0.3 barn. The consistent values of $\overline{\sigma}_{C_p}$ are obtained from figure 5(b) as $\overline{\sigma}_{C_p}$ = 0.020±0.020 barn for gold sphere 1 and $\overline{\sigma}_{C_p}$ = 0.040±0.015 barn for gold sphere 2.

The uncertainties in $\overline{\sigma}_{C_s}$ resulting from uncertainties in the resonance parameters that are used as input data to the Monte Carlo analysis are calculated separately, as they were with iodine. The effects on $\overline{\sigma}_{C_s}$ of an estimated 10-percent uncertainty in $\overline{\Gamma}_\gamma$ and the measured uncertainties in $\overline{\Gamma}_n$ and $\overline{D}$ were evaluated by performing separate Monte Carlo calculations.

Interpretation of the sphere transmission experiments for both gold spheres, which is consistent with the measured average total cross section and the known s-wave resonance parameters, provides the following cross sections: σ_{pot} = 8.7±0.3 barn; $\overline{\sigma}_{C_s}$ = 0.665±0.050 barn; $\overline{\sigma}_{C_p}$ = 0.035±0.013 barn; and $\overline{\sigma}_C$ = 0.700±0.050 barn.

Implications for Other Elements

Sphere transmission data (ref. 1) for five elements, iodine, gold, indium, antimony, and silver, and results that were updated by Schmitt in reference 7 for new experimental values of average total cross section $\overline{\sigma}_T$ are shown in table VI (p. 16). The values of $\overline{\sigma}_T$ used and the resulting values of $\overline{\sigma}_C$ obtained by the Bethe method of analysis are compared with the present Monte Carlo results in table VIII. In applying the Bethe

TABLE VIII. - AVERAGE CROSS SECTIONS AND RESONANCE PARAMETERS AT 24 KEV

Element	Total cross section, $\bar{\sigma}_T$, b	Average capture cross section, $\bar{\sigma}_C$, mb			Potential scattering cross section, σ_{pot}, b		Average s-wave resonance scattering component,[a] $\bar{\sigma}_{S_s}$, b	Average radiation width, $\bar{\Gamma}_\gamma$, eV	Average neutron width, $\bar{\Gamma}_n$, eV	Average s-wave level spacing, $\bar{D}$, eV
		Values of Schmitt corrected for resonance self-protection	Present Monte Carlo results	Bethe method using σ_{pot} as effective scattering cross section	Values of Duke compilation	Present Monte Carlo results				
Gold	13.67±0.28	532±60	700±50	650	9.3±0.3	8.7±0.3	4.3	0.170	0.760	17
Iodine	6.69±0.36	768±90	800±80	840	4.2±0.3	4.0±0.3	1.9	.107	.280	13
Indium	6.11±0.18	854±60	------	860	4.4±0.4	-------	.9	.080	.140	9
Antimony	5.99±0.14	578±45	------	600	3.6±0.4	-------	1.8	.080	.340	22
Silver	7.85±0.23	1127±80	------	1110	5.4±0.5	-------	1.3	.148	.220	18

[a] $\bar{\sigma}_{S_s} = \bar{\sigma}_T - \bar{\sigma}_C - \sigma_{pot}$.

method, Schmitt employed the difference between $\bar{\sigma}_T$ and $\bar{\sigma}_C$ as the average effective scattering cross section $\bar{\sigma}_S$ to solve for the value of $\bar{\sigma}_C$ that satisfied the observed sphere transmission data in an iterative calculation. Resonance self-protection (RSP) corrections were then applied to these results, and the indicated values of $\bar{\sigma}_C$ were increased by factors as large as 15 percent. If large s-wave resonance scattering contributions are present, the simple difference between $\bar{\sigma}_T$ and $\bar{\sigma}_C$ does not represent the effective value of $\bar{\sigma}_S$ to be used in the Bethe analysis. The use of this difference has resulted in large underestimates in $\bar{\sigma}_C$ for gold and can result in errors for other elements.

Also shown in table VIII are the results of calculations by the Bethe method in which the value of $\bar{\sigma}_S$ was taken to be equal to σ_{pot}. The question as to what constitutes the effective value of $\bar{\sigma}_S$ is crucial to the application of the Bethe analysis to sphere transmission data at 24 keV. Considering the uniqueness of the resonance structure for each element, it is difficult to establish a criterion for finding an effective value of $\bar{\sigma}_S$. As is seen from table VIII, values of $\bar{\sigma}_C$ obtained by applying the Bethe analysis to the sphere transmission data when σ_{pot} is employed as the effective scattering cross section are in reasonable agreement with the Monte Carlo results for gold and iodine. The results obtained for indium, antimony, and silver by using σ_{pot} are in agreement with results reported by Schmitt (ref. 7) that have been corrected for RSP. When σ_{pot} is used, there is no necessity for invoking any RSP correction.

Values of σ_{pot} were obtained as

$$\sigma_{pot} = 4\pi(R')^2$$

where the values of the effective nuclear radii R' were taken from a listing of neutron strength functions compiled at Duke University and presented in reference 12. The values of σ_{pot} are shown in table VIII; values of σ_{pot} for gold and iodine obtained from the present Monte Carlo analysis are in good agreement with the Duke values.

An estimate of the relative s-wave scattering contributions $\bar{\sigma}_{S_s}$ may be obtained as $\bar{\sigma}_{S_s} = \bar{\sigma}_T - \bar{\sigma}_C - \sigma_{pot}$. Values of $\bar{\sigma}_{S_s}$ are shown in table VIII and indicate the large resonance scattering contribution to $\bar{\sigma}_T$ for gold.

It has been shown that the unusually large average neutron width $\bar{\Gamma}_n$ for gold introduces relatively large scattering components to the resonance cross sections, which can make the Bethe analysis invalid and the RSP corrections approximate. For gold, the s-wave contribution is dominant with a small p-wave contribution required, so that the effects of s-wave resonance scattering in thick gold spheres are large.

For the case of iodine, which has a smaller average neutron width $\bar{\Gamma}_n$ than gold and for which the s-wave and p-wave contributions to $\bar{\sigma}_C$ are about equal, the effects of

s-wave resonance scattering are smaller than for gold. The parameters $\overline{\Gamma}_\gamma$, $\overline{\Gamma}_n$, and $\overline{D}$ that have been measured for silver (ref. 10) and estimated for indium and antimony (ref. 13) are similar to those of iodine, so that s-wave resonance scattering constitutes smaller perturbations to the total cross section than for gold.

From the foregoing results, reasonable values of $\overline{\sigma}_C$ have been obtained by the Bethe method of sphere transmission experiment analysis at 24 keV with the potential scattering cross section used to represent the effective scattering cross section. The case of gold indicates that difficulties exist with the interpretation of sphere transmission measurements at 24 keV without a priori knowledge of average s-wave resonance parameters for the nuclei being studied.

SUMMARY OF RESULTS

Sphere transmission experiments for measuring values of average capture cross sections $\overline{\sigma}_C$ at 24 keV have been analyzed in the past by the Bethe method, which assumes capture and scattering cross sections to be independent of energy. Monte Carlo calculations for transmission through thick spheres are compared with the Bethe solutions for cross sections with periodic step changes in capture and scattering superimposed on constant potential scattering cross sections. The two methods agree for constant cross sections, but the Bethe method increasingly underestimates $\overline{\sigma}_C$ for larger step changes in cross section.

For interpretation of sphere transmission experiments, the present Monte Carlo method was adapted to calculate the average s-wave and p-wave contributions to $\overline{\sigma}_C$. The statistical results from slow neutron resonance spectroscopy were used as input data. The program uses Doppler-broadened Breit-Wigner resonances with a Porter-Thomas distribution of neutron widths and a Wigner distribution of level spacings to obtain microscopic cross sections for s-wave levels. Average p-wave contributions are approximated as an additive constant to the average s-wave capture cross section.

The Monte Carlo method was applied to published 24-keV transmission data for gold and iodine. For gold, $\overline{\sigma}_C$ was calculated to be 700±50 millibarns, which includes a small p-wave contribution. This is to be compared with a reported value of 532±60 millibarns that includes a correction for RSP in the thick spheres used. The potential scattering cross section for gold was determined herein as 8.7±0.3 barn. For iodine, the s-wave and p-wave contributions were determined to be 442±50 and 358±60 millibarns, respectively, for a value of $\overline{\sigma}_C$ of 800±80 millibarns; this is in substantial agreement with a reported value of 768±90 millibarns. The potential scattering cross section for iodine was determined herein as 4.0±0.3 barn.

For nuclei with large s-wave resonance scattering cross sections such as gold, the

Bethe method of analysis for sphere transmission experiments encounters difficulties because of ambiguity as to the value of the effective scattering cross section to be used. Values of $\overline{\sigma}_C$ obtained by the Bethe method are found to be in good agreement with the Monte Carlo results if the potential scattering cross section is used to represent the effective scattering cross section. It is possible that the Bethe method can still be employed for interpretation of sphere transmission experiments in the absence of spectroscopic data and without the necessity of invoking resonance self-protection corrections, providing the potential scattering cross section is used.

Lewis Research Center,
National Aeronautics and Space Administration,
Cleveland, Ohio, March 17, 1966.

REFERENCES

1. Schmitt, H. W.; and Cook, C. W.: Absolute Neutron Absorption Cross Sections for Sb-Be Photoneutrons. Nucl. Phys., vol. 20, Oct. 4, 1960, pp. 202-219.

2. Gibbons, J. H.; Macklin, R. L.; Miller, P. D.; and Neiler, J. H.: Average Radiative Capture Cross Sections for 7- to 170-kev Neutrons. Phys. Rev., vol. 122, no. 1, Apr. 1, 1961, pp. 182-201.

3. Gibbons, J. H.: Neutron Radiative Capture Reactions. Progress in Fast Neutron Physics, G. C. Phillips, J. B. Marion, and J. R. Risser, eds., Univ. Chicago Press, 1963, pp. 193-212.

4. Bogart, Donald: Boron Cross Sections as a Source of Discrepancy for Capture Cross Sections in the keV Range. NASA TR R- , 1966.

5. Schmitt, H. W.: Determination of the Energy of Antimony-Beryllium Photoneutrons. Nucl. Phys., vol. 20, Oct. 4, 1960, pp. 220-226.

6. Bethe, H. A.; Beyster, J. R.; and Carter, R. E.: Inelastic Cross-Sections for Fission-Spectrum Neutrons, I. J. Nucl. Energy, vol. 3, 1956, pp. 207-223.

7. Schmitt, H. W.: Remarks on Absolute Heavy-Element Neutron Capture Cross Sections Determined by the Sphere Transmission Method. Rept. No. EANDC-33U, Atomic Weapons Res. Estab. (Gt. Brit.), 1963, pp. 41-43.

8. Everett, C. J.; Cashwell, E. D.; and Rechard, O. W.: A Monte Carlo Determination of the Escape Fraction for a Scattering Spherical Shell with Central Point Source. Rept. No. LA-1583, Los Alamos Sci. Lab., Aug. 24, 1953.

9. Garg, J. B.; Rainwater, J.; and Havens, W. W., Jr.: Neutron Resonance Spectroscopy. V. Nb, Ag, I, and Cs. Phys. Rev., vol. 137, no. 3B, Feb. 8, 1965, pp. B547-B575.

10. Desjardins, J. S.; Rosen, J. L.; Havens, W. W., Jr.; and Rainwater, J.: Slow Neutron Resonance Spectroscopy. II. Ag, Au, Ta. Phys. Rev., vol. 120, no. 6, Dec. 15, 1960, pp. 2214-2226.

11. Joanou, G. D.; and Dudek, J. S.: GAM-II. A B_3 Code for the Calculation of Fast-Neutron Spectra and Associated Multigroup Constants. Rept. No. GA-4265, General Dynamics Corp., Sept. 16, 1963.

12. Smith, A. B., Compiler: The AEC Nuclear Cross Sections Advisory Group Meeting at Columbia University, June 4-5, 1964. Rept. No. WASH-1048 (sec. 5, Duke Univ.), AEC, 1964, p. 32.

13. Hughes, D. J.; Magurno, B. A.; and Brussel, M. K.: Neutron Cross Sections. Rept. No. BNL-325, Second ed., Suppl. I, AEC, Jan. 1, 1960.

"The aeronautical and space activities of the United States shall be conducted so as to contribute . . . to the expansion of human knowledge of phenomena in the atmosphere and space. The Administration shall provide for the widest practicable and appropriate dissemination of information concerning its activities and the results thereof."

—NATIONAL AERONAUTICS AND SPACE ACT OF 1958

NASA SCIENTIFIC AND TECHNICAL PUBLICATIONS

TECHNICAL REPORTS: Scientific and technical information considered important, complete, and a lasting contribution to existing knowledge.

TECHNICAL NOTES: Information less broad in scope but nevertheless of importance as a contribution to existing knowledge.

TECHNICAL MEMORANDUMS: Information receiving limited distribution because of preliminary data, security classification, or other reasons.

CONTRACTOR REPORTS: Technical information generated in connection with a NASA contract or grant and released under NASA auspices.

TECHNICAL TRANSLATIONS: Information published in a foreign language considered to merit NASA distribution in English.

TECHNICAL REPRINTS: Information derived from NASA activities and initially published in the form of journal articles.

SPECIAL PUBLICATIONS: Information derived from or of value to NASA activities but not necessarily reporting the results of individual NASA-programmed scientific efforts. Publications include conference proceedings, monographs, data compilations, handbooks, sourcebooks, and special bibliographies.

Details on the availability of these publications may be obtained from:

SCIENTIFIC AND TECHNICAL INFORMATION DIVISION

NATIONAL AERONAUTICS AND SPACE ADMINISTRATION

Washington, D.C. 20546